

Higgs-mass dependence of the effective electroweak mixing angle $\sin^2 \theta_{\text{eff}}$ at the two-loop level

W. HOLLIK, U. MEIER and S. UCCIRATI *

Max-Planck-Institut für Physik
(Werner-Heisenberg-Institut)
D-80805 München, Germany

Abstract

The result for the Higgs-dependent electroweak two-loop bosonic contributions to the effective leptonic mixing angle of the Z -boson in the Standard Model is presented. Together with the previously calculated fermionic contributions it yields the complete dependence of $\sin^2 \theta_{\text{eff}}$ on the Higgs-boson mass M_H . Compared to the fermionic contributions, the bosonic contributions are found to be smaller and have the opposite sign, compensating part of the fermionic contributions.

*Address after October 3 2005, INFN Sezione di Torino, Italy

1 Introduction

The effective electroweak mixing angle for leptons, $\sin^2 \theta_{\text{eff}}$, is experimentally determined with high accuracy from measurements of various asymmetries on the Z resonance, with the current value 0.23153 ± 0.00016 [1], and further improvements are expected from future collider experiments [2, 3]. Analyses done in combination with the theoretical predictions for $\sin^2 \theta_{\text{eff}}$ in the Standard Model yield stringent bounds on the Higgs-boson mass M_H , making $\sin^2 \theta_{\text{eff}}$ a precision observable of central importance for tests of the Standard Model. Therefore, a precise and reliable calculation is a necessity, requiring at least the complete electroweak two-loop contributions.

$\sin^2 \theta_{\text{eff}}$ is determined from the ratio of the dressed vector and axial vector couplings $g_{V,A}$ of the Z boson to leptons [4],

$$\sin^2 \theta_{\text{eff}} = \frac{1}{4} \left(1 - \text{Re} \frac{g_V}{g_A} \right). \quad (1)$$

It is related to the vectorboson-mass ratio or the on-shell quantity s_W^2 , respectively, via

$$\sin^2 \theta_{\text{eff}} = \kappa s_W^2 = \kappa \left(1 - \frac{M_W^2}{M_Z^2} \right), \quad \kappa = 1 + \Delta\kappa, \quad (2)$$

involving the κ factor, which is unity at the tree level and accommodates the higher-order contributions in $\Delta\kappa$. In recent independent calculations the complete two-loop electroweak corrections of the fermionic type, i.e. with at least one closed fermion loop, to $\Delta\kappa$ were obtained [5, 6]. The bosonic two-loop corrections, however, are still missing. In this note we present a first step towards the full $\mathcal{O}(\alpha^2)$ result for $\Delta\kappa$, namely the results of the subclass of Higgs dependent contributions, thus providing the complete Higgs-boson mass dependence of the bosonic two-loop corrections.

2 Structure of electroweak two-loop contributions

The general strategy of our calculation of the two-loop electroweak contributions to $\sin^2 \theta_{\text{eff}}$, including renormalization, has been described in [6]. As outlined in [6], one has to take into account basically the classes of diagrams depicted schematically in Fig. 1, where the circles denote renormalized two- and three-point irreducible vertex functions at the one-loop level in Fig. 1a and at two-loop order in Fig. 1c and 1d.

The real part of the diagram shown in Fig. 1c vanishes in the on-shell renormalization scheme [7] adopted in our calculation and the diagrams of Fig. 1a and 1b only contribute products of imaginary parts of one-loop functions. So we are left with the irreducible two-loop $Z\ell\ell$ -vertex diagrams in Fig. 1d. The Z couplings in (1) appear in the renormalized $Z\ell\ell$ vertex for on-shell Z bosons,

$$\hat{\Gamma}_\mu^{Z\ell\ell(2)}(M_Z^2) = \gamma_\mu (g_V - g_A \gamma_5). \quad (3)$$

As for the fermionic corrections, we split the two-loop contribution for the renormalized vertex into two UV-finite pieces according to

$$\begin{aligned}\hat{\Gamma}_\mu^{Z\ell\ell(2)}(M_Z^2) &= \Gamma_\mu^{Z\ell\ell(2)}(M_Z^2) + \Gamma_\mu^{CT} \\ &= [\Gamma_\mu^{Z\ell\ell(2)}(0) + \Gamma_\mu^{CT}] + [\Gamma_\mu^{Z\ell\ell(2)}(M_Z^2) - \Gamma_\mu^{Z\ell\ell(2)}(0)] .\end{aligned}\quad (4)$$

$\Gamma_\mu^{Z\ell\ell(2)}(P^2)$ denotes the corresponding unrenormalized $Z\ell\ell$ vertex for on-shell leptons and momentum transfer P^2 , and Γ_μ^{CT} is the two-loop counter term, which is independent of P^2 . The first term in the decomposition of (4) therefore contains the complete two-loop renormalization, but no genuine two-loop vertex diagrams since in absence of external momenta they reduce to simpler vacuum integrals. All the genuine two-loop vertex diagrams appear as subtracted quantities in the second term in (4).

As a first step towards the complete bosonic two-loop corrections, we consider the

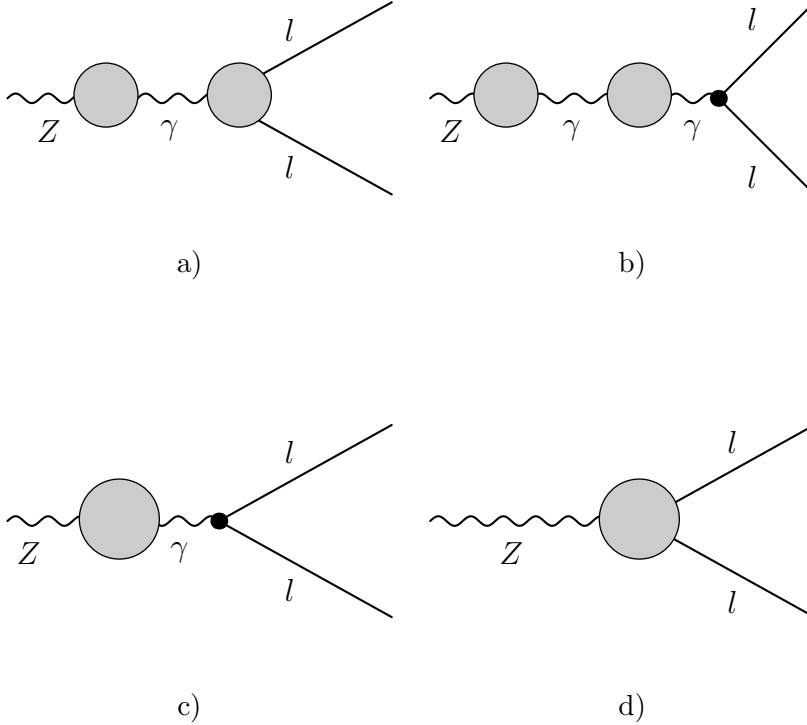


Figure 1: Generic classes of two loop diagrams

Higgs-mass dependence. To this end we calculate the subtracted two-loop bosonic $\Delta\kappa_{bos}^{(\alpha^2)}$,

$$\Delta\kappa_{bos,sub}^{(\alpha^2)} = \Delta\kappa_{bos}^{(\alpha^2)}(M_H) - \Delta\kappa_{bos}^{(\alpha^2)}(M_H^0), \quad (5)$$

for a fixed reference mass of the Higgs boson, chosen as $M_H^0 = 100$ GeV. The quantity $\Delta\kappa_{bos,sub}^{(\alpha^2)}$ is UV finite and gauge-parameter independent. The dependence on M_H enters exclusively through diagrams with internal Higgs boson lines. Some typical examples are displayed in Fig. 2.

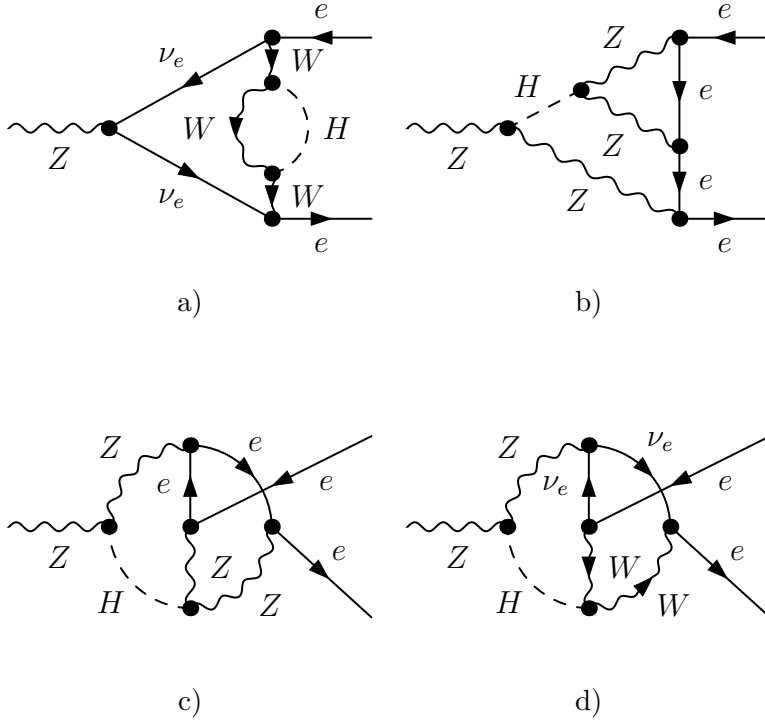


Figure 2: Examples of diagrams containing internal Higgs bosons

The computation of the renormalized vertex at $P^2 = 0$ [first term in (4)] can be done in analogy to the fermionic case [6], which means generating Feynman diagrams with *FeynArts* [8] and applying *TwoCalc* [9] to reduce the amplitudes to standard integrals. The resulting scalar one-loop integrals and two-loop vacuum integrals are calculated using known analytic results [10, 11]. The two-loop self-energies with non-vanishing external momentum, as part of the two-loop counterterm, are obtained with the help of one-dimensional integral representations [12]. Moreover, we implemented new methods described in [13], and used them for cross checks.

For the subtracted vertex, the second term in equation (4), two independent calculations were performed, based either on *FeynArts* or on *GraphShot* [14] for generating the vertex amplitudes. The diagrams containing self-energy subloops (e.g. Fig. 2a) were evaluated using the method of one-dimensional integral representations, as described in [6]. In addition, as an independent check, the methods described in [13] were implemented and applied. The diagrams containing vertex subloops (e.g. Fig. 2b) were also calculated as in the fermionic case, using the methods described in [13]. The only new type of diagrams compared to the fermionic case are the two non-planar diagrams in Fig. 2c,d. The method used for their evaluation is explained in the next section.

3 Non-planar diagrams

The non-planar diagrams in Fig. 2c,d are UV-finite and can be evaluated in 4 dimensions. We have to deal with diagrams of the type

$$V_{222}^{(\mu,\mu\nu)} = \int d^4 q_1 \int d^4 q_2 \frac{(q_1^\mu, q_1^\mu q_1^\nu)}{[1][2][3][4][5][6]}, \quad (6)$$

with the following short-hand notation for the propagators,

$$\begin{aligned} [1] &= q_1^2 - M_V^2, & [2] &= (q_1 - p_1)^2, & [3] &= (q_1 - q_2 + p_1)^2 - M_H^2, \\ [4] &= (q_1 - q_2 - p_2)^2 - M_Z^2, & [5] &= q_2^2, & [6] &= (q_2 - p_1)^2 - M_V^2; \\ M_V &= (M_W, M_Z). \end{aligned} \quad (7)$$

Following the discussion given in [13], we first combine the propagators [1] and [2] with a Feynman-parameter z_1 , the propagators [3] and [4] with a Feynman-parameter z_2 and the propagators [5] and [6] with a Feynman-parameter z_3 . Then we change variables according to $q_1 \rightarrow q_1 + z_1 p_2$, $q_2 \rightarrow q_2 + z_3 p_1$ and combine the q_1 and $q_1 - q_2$ propagators with a parameter x . After the q_1 -integration we combine the residual propagators with a parameter y and carry out the q_2 integration.

Since we consider the external fermions to be massless we have $p_{1,2}^2 = 0$. In this situation, the expression for V_{222} is much simpler than in the general case because we have just to deal with integrals of the type

$$\int_0^1 dx dy dz_1 dz_2 dz_3 z_3^n (a z_1 z_3 + b z_3 + c z_1 + d)^{-2} \quad (8)$$

with $n = 0, 1, 2$. a,b,c,d are functions of the internal masses, of the external Z momentum and of the parameters x, y, z_2 , but they are independent of z_1 and z_3 . For $n = 0$ we perform the integrations in z_1 and z_3 analytically,

$$\int_0^1 dz_1 dz_3 (a z_1 z_3 + b z_3 + c z_1 + d)^{-2} = \frac{1}{ad - bc} \ln \left(1 + \frac{ad - bc}{(c + d)(b + d)} \right), \quad (9)$$

whereas for $n = 1, 2$ the z_1 integration and an integration by parts in z_3 are done analytically,

$$\int_0^1 dz_1 dz_3 z_3^n (a z_1 z_3 + b z_3 + c z_1 + d)^{-2} = \int_0^1 dz_3 \frac{n z_3^{n-1}}{ad - bc} \ln \left(1 + \frac{(1 - z_3)(ad - bc)}{((a + b) z_3 + c + d)(b + d)} \right). \quad (10)$$

In both cases smooth integrands are obtained, suitable for follow-up numerical integrations. The algebraic handling and the numerical evaluation were performed in two independent computations for cross-checking the results. For the numerical integration the NAG library D01GDF [15] was used in one case and the CUBA library [16] in the other case.

4 Results

The evaluation and presentation of the final result are done for the set of input parameters put together in Tab. 1. M_W and M_Z are the experimental values of the W - and Z -boson masses [17], which are the on-shell masses. They have to be converted to the values in the pole mass scheme [7], labeled as \overline{M}_W and \overline{M}_Z , which are used internally for the calculation. These quantities are related via $M_{W,Z} = \overline{M}_{W,Z} + \Gamma_{W,Z}^2 / (2 M_{W,Z})$. For Γ_Z the experimental value (Tab. 1) and for Γ_W the theoretical value has been used, *i.e.* $\Gamma_W = 3 G_\mu M_W^3 / (2\sqrt{2}\pi) (1 + 2\alpha_s (M_W^2) / (3\pi))$ with sufficient accuracy.

parameter	value
M_W	80.426 GeV
M_Z	91.1876 GeV
Γ_Z	2.4952 GeV
m_t	178.0 GeV
$\Delta\alpha(M_Z^2)$	0.05907
$\alpha_s(M_Z^2)$	0.117
G_μ	1.16637×10^{-5}
\overline{M}_W	80.3986 GeV
\overline{M}_Z	91.1535 GeV

Table 1: Input parameters entering our computation. M_W and M_Z are the experimental values of the W - and Z -boson masses, whereas \overline{M}_W and \overline{M}_Z are the calculated quantities in the pole mass scheme.

The results are given for $\Delta\kappa$, eq. (2), and are listed in Tab. 2 for different values of M_H . For comparison, Tab. 2 also contains the values of the fermionic corrections and the corresponding subtracted quantity $\Delta\kappa_{ferm,sub}^{(\alpha^2)} = \Delta\kappa_{ferm}^{(\alpha^2)}(M_H) - \Delta\kappa_{ferm}^{(\alpha^2)}(M_H^0)$.

In the considered range of the Higgs-boson mass, the bosonic result has the opposite sign and is thus compensates part of the fermionic contributions, which could be

$M_H [GeV]$	$\Delta\kappa_{ferm}^{(\alpha^2)} \times 10^{-4}$	$\Delta\kappa_{ferm,sub}^{(\alpha^2)} \times 10^{-4}$	$\Delta\kappa_{bos,sub}^{(\alpha^2)} \times 10^{-4}$
100	-0.637(1)	0	0
200	-2.165(1)	-1.528	0.265
600	-5.012(1)	-4.375	0.914
1000	-4.737(1)	-4.100	1.849

Table 2: Two-loop result for $\Delta\kappa$ in comparison with the fermionic contributions

important for the precision expected from the GigaZ mode of the ILC. The uncertainties from numerical integration in the bosonic result are of the order 10^{-9} and hence negligible.

At the end, according to (2), the final M_H -dependence of $\sin^2 \theta_{\text{eff}}$ is obtained in combination with $M_W(M_H)$ derived from G_μ and Δr [18]. The two contributions, from M_W and κ , have different sign and cancel each other to a large extend, as illustrated in Tab. 3.

$M_H [GeV]$	$\Delta M_{W,bos}^{(\alpha^2)} [MeV][18]$	$\sin^2 \theta_{\text{eff}}^{sub} (\Delta M_W) \times 10^{-5}$	$\sin^2 \theta_{\text{eff}}^{sub} (\Delta\kappa) \times 10^{-5}$
100	-1.0	0	0
200	-0.5	-0.97	0.59
600	-0.1	-1.74	2.03
1000	0.6	-3.10	4.11

Table 3: Variation of $\sin^2 \theta_{\text{eff}}$ originating from $M_W(M_H)$ (column 3) in comparison with the variation resulting from $\Delta\kappa$. Column 2 contains the bosonic 2-loop contributions to M_W from [18].

In conclusion, we have evaluated the bosonic electroweak 2-loop corrections to $\sin^2 \theta_{\text{eff}}$ containing internal Higgs bosons. As a new feature, non-planar vertex diagrams appear, and a method to calculate such non-planar diagrams has been described. Our numerical result for $\Delta\kappa^{(\alpha^2)}$ shows that the Higgs-mass dependence of the two-loop prediction for $\Delta\kappa$ is affected by the bosonic contributions compensating almost the corresponding contribution to $\sin^2 \theta_{\text{eff}}$ induced by the bosonic 2-loop corrections to $M_W(M_H)$. Hence, without the bosonic $\Delta\kappa$ contributions, the variation of $\sin^2 \theta_{\text{eff}}$ with M_H through the W mass alone would go into the wrong direction.

S.U. would like to express his gratitude to Stefano Actis for making available the beta version of GraphShot, a FORM code for generating and reducing standard model one- and two-loop diagrams which is presently under development at Torino University.

References

- [1] The LEP Collaborations, the LEP Electroweak Working Group, the SLD Electroweak and Heavy Flavour Groups, arXiv:hep-ex/0509008.
- [2] J. A. Aguilar-Saavedra *et al.*, TESLA Technical Design Report Part III: *Physics at an e^+e^- Linear Collider* [hep-ph/0106315]. T. Abe *et al.* [American Linear Collider Working Group Collaboration], in *Proc. of the APS/DPF/DPB Summer Study on the Future of Particle Physics (Snowmass 2001)* ed. R. Davidson and C. Quigg, SLAC-R-570, *Resource book for Snowmass 2001* [hep-ex/0106055, hep-ex/0106056, hep-ex/0106057, hep-ex/0106058]. K. Abe *et al.* [ACFA Linear Collider Working Group Collaboration], ACFA Linear Collider Working Group report, [hep-ph/0109166].
- [3] U. Baur, R. Clare, J. Erler, S. Heinemeyer, D. Wackeroth, G. Weiglein and D. R. Wood, in *Proc. of the APS/DPF/DPB Summer Study on the Future of Particle Physics (Snowmass 2001)* ed. N. Graf, eConf **C010630** (2001) P122 [arXiv:hep-ph/0111314].
- [4] D. Y. Bardin *et al.*, hep-ph/9709229, in *Precision Calculations for the Z Resonance*, D. Bardin, W. Hollik, G. Passarino (Eds.), CERN 95-03.
- [5] M. Awramik, M. Czakon, A. Freitas and G. Weiglein, Phys. Rev. Lett. **93** (2004) 201805 [arXiv:hep-ph/0407317], Nucl. Phys. Proc. Suppl. **135** (2004) 119 [arXiv:hep-ph/0408207].
- [6] W. Hollik, U. Meier and S. Uccirati, arXiv:hep-ph/0507158.
- [7] A. Freitas, W. Hollik, W. Walter and G. Weiglein, Phys. Lett. B **495** (2000) 338, E: ibid. B **570** (2003) 260 [hep-ph/0007091] and Nucl. Phys. B **632** (2002) 189, E: ibid. B **666** (2003) 305 [hep-ph/0202131].
- [8] J. Küblbeck, M. Böhm and A. Denner, Comp. Phys. Comm. **60** (1990) 165. T. Hahn, Nucl. Phys. Proc. Suppl. **89** (2000) 231 [arXiv:hep-ph/0005029], Comput. Phys. Commun. **140** (2001) 418 [arXiv:hep-ph/0012260], *FeynArts User's Guide*, available at <http://www.feynarts.de>.
- [9] G. Weiglein, R. Scharf and M. Böhm, Nucl. Phys. B **416** (1994) 606 [arXiv:hep-ph/9310358]; G. Weiglein, R. Mertig, R. Scharf and M. Böhm, PRINT-95-128 *Prepared for 2nd International Workshop on Software Engineering, Artificial Intelligence and Expert Systems for High-energy and Nuclear Physics, La Londe Les Maures, France, 13-18 Jan 1992*
- [10] G. 't Hooft and M. J. G. Veltman, Nucl. Phys. B **153** (1979) 365.
- [11] A. I. Davydychev and J. B. Tausk, Nucl. Phys. B **397** (1993) 123.

- [12] S. Bauberger, M. Böhm, G. Weiglein, F. A. Berends and M. Buza, Nucl. Phys. Proc. Suppl. **37B** (1994) 95 [arXiv:hep-ph/9406404]; S. Bauberger, F. A. Berends, M. Böhm and M. Buza, Nucl. Phys. B **434** (1995) 383 [arXiv:hep-ph/9409388]; S. Bauberger and M. Böhm, Nucl. Phys. B **445** (1995) 25 [arXiv:hep-ph/9501201].
- [13] A. Ferroglia, M. Passera, G. Passarino and S. Uccirati, Nucl. Phys. B **680** (2004) 199 [arXiv:hep-ph/0311186] and Nucl. Phys. B **650** (2003) 162 [arXiv:hep-ph/0209219]; S. Actis, A. Ferroglia, G. Passarino, M. Passera and S. Uccirati, Nucl. Phys. B **703** (2004) 3 [arXiv:hep-ph/0402132]; G. Passarino, Nucl. Phys. B **619** (2001) 257 [arXiv:hep-ph/0108252]; G. Passarino and S. Uccirati, Nucl. Phys. B **629** (2002) 97 [arXiv:hep-ph/0112004]; S. Uccirati, Acta Phys. Polon. B **35** (2004) 2573 [arXiv:hep-ph/0410332].
- [14] S. Actis, A. Ferroglia, G. Passarino and M. Passera, *GraphShot*, a FORM package for generating, reducing and evaluating one and two loop Feynman diagrams (in preparation).
- [15] NAG Fortran Library, Mark 19, The Numerical Algorithms Group Ltd, Oxford UK. 1999.
- [16] T. Hahn, arXiv:hep-ph/0404043.
- [17] S. Eidelman et al. [Particle Data Group], Phys. Lett. B **592** (2004) 1.
- [18] M. Awramik and M. Czakon, Phys. Rev. Lett. **89** (2002) 241801 [hep-ph/0208113]. A. Onishchenko and O. Veretin, Phys. Lett. B **551** (2003) 111 [hep-ph/0209010]. M. Awramik, M. Czakon, A. Onishchenko and O. Veretin, Phys. Rev. D **68**, 053004 (2003) [hep-ph/0209084].